PROCEEDINGS B

royalsocietypublishing.org/journal/rspb

Research

Cite this article: Machado FA, Marroig G, Hubbe A. 2022 The pre-eminent role of directional selection in generating extreme morphological change in glyptodonts (Cingulata; Xenarthra). *Proc. R. Soc. B* **289**: 20212521.
https://doi.org/10.1098/rspb.2021.2521

Received: 18 November 2021
Accepted: 14 December 2021

Subject Category:
Palaeobiology

Subject Areas:
palaeontology, evolution

Keywords:
skull, extreme morphology, fossil, natural selection, rates of evolution

Authors for correspondence:
Fabio A. Machado
e-mail: fmachado@vt.edu
Gabriel Marroig
e-mail: gmarroig@usp.br
Alex Hubbe
e-mail: alexhubbe@yahoo.com

Electronic supplementary material is available online at https://doi.org/10.6084/m9.figshare.c.5772149.

THE ROYAL SOCIETY PUBLISHING

The pre-eminent role of directional selection in generating extreme morphological change in glyptodonts (Cingulata; Xenarthra)

Fabio A. Machado[1], Gabriel Marroig[2] and Alex Hubbe[3]

[1]Department of Biology, Virginia Tech, Blacksburg, USA
[2]Departamento de Genética e Biologia Evolutiva, Instituto de Biociências, Universidade de São Paulo, São Paulo, SP, Brazil
[3]Departamento de Oceanografia, Instituto de Geociências, Universidade Federal da Bahia, Salvador, Brazil

FAM, 0000-0002-0215-9926; AH, 0000-0002-3226-0144

The prevalence of stasis on macroevolution has been classically taken as evidence of the strong role of stabilizing selection in constraining morphological change. Rates of evolution calculated over longer timescales tend to fall below the expected under genetic drift, suggesting that directional selection signals are erased at longer timescales. Here, we investigated the rates of morphological evolution of the skull in a fossil lineage that underwent extreme morphological modification, the glyptodonts. Contrary to what was expected, we show here that directional selection was the primary process during the evolution of glyptodonts. Furthermore, the reconstruction of selection patterns shows that traits selected to generate a glyptodont morphology are markedly different from those operating on extant armadillos. Changes in both direction and magnitude of selection are probably tied to glyptodonts' invasion of a specialist-herbivore adaptive zone. These results suggest that directional selection might have played a more critical role in the evolution of extreme morphologies than previously imagined.

1. Introduction

Identifying signals of adaptive evolution using rates of change on a macroevolutionary scale is inherently problematic because tempo and mode of evolution are intertwined. While stabilizing selection slows down phenotypic change, directional selection can produce faster rates of evolution [1–3]. This means that the action of selection (directional or stabilizing) can be identified by contrasting how fast species evolve to the expected rates under genetic drift [1,2]. While this framework has been successfully applied to microevolutionary timescales [4], its usefulness to macroevolutionary and deep-time studies has been contentious [5].

At larger timescales, it is challenging to quantify the effect of directional selection on the evolutionary process. The leading mechanism of phenotypic evolution on the macroevolutionary scale is thought to be stabilizing selection, as attested by the prevalence of stasis in the fossil record [6]. This does not necessarily mean that directional selection did not play any role in phenotypic diversification. Because the adaptive landscape (the relationship between phenotype and fitness) is thought to be rugged, with many different optimal phenotypic combinations (peaks), evolutionary change under directional selection is bound to be fast during peak shifts and punctuated at the macroevolutionary scale (figure 1). Thus, because stasis is so prevalent and measured rates of change reflect the net-evolutionary processes that operated during lineages' histories, rates of evolution calculated on phylogenies and fossil record tend to be small compared to rates observed in extant populations [5]. As a result, measured net-evolutionary rates of morphological change are more commonly than not consistent with

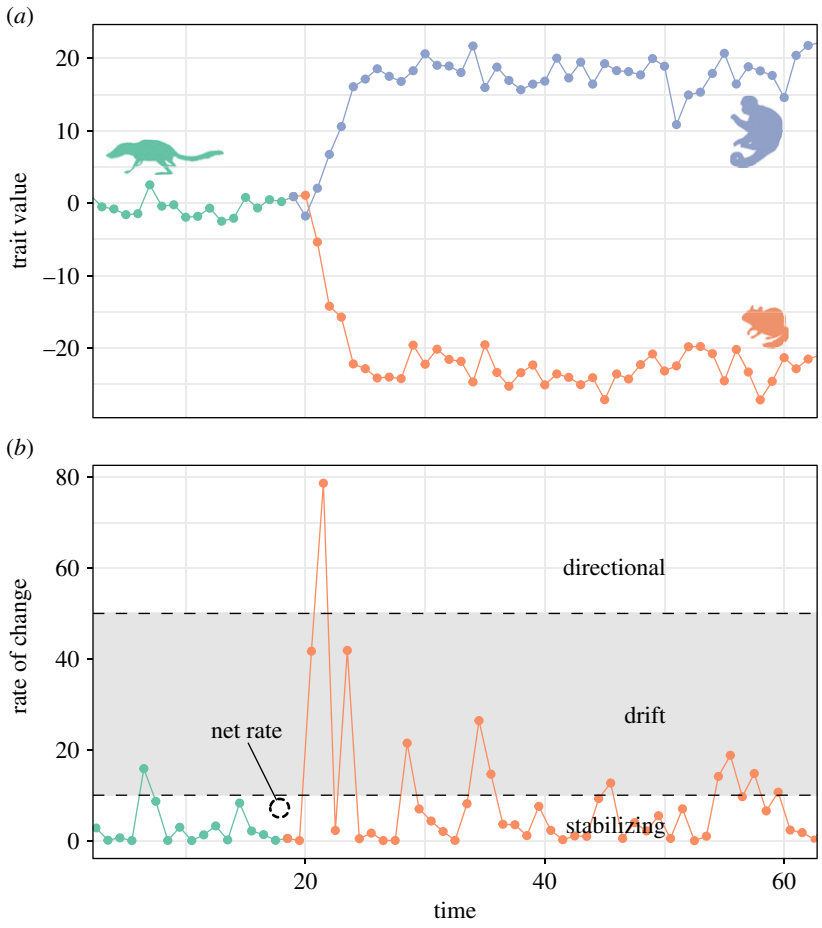

Figure 1. (*a*) Evolution of a trait in an ancestral population (green) and during cladogenesis caused by a peak shift, resulting in two daughter lineages (blue and orange). (*b*) Rates of evolution of the trait depicted in (*a*) for the ancestral species and one of the daughter lineages. The grey band represents the rates of evolution consistent with the expectation under genetic drift. Values above it are produced by directional selection and values below it by stabilizing selection. Even though the linage experienced expressive directional selection, in practice, one calculates net rates of evolution over the whole period since the origin of the species (dashed dot), which tend to be small and consistent with the expected under stabilizing selection. (Online version in colour.)

evolution under stabilizing selection or drift [5,7–9]. This probably explains why macroevolutionary studies usually infer the action of directional selection indirectly through pattern-based methods rather than adopting biologically informed models (e.g., those derived from quantitative genetics theory).

While this departure from a biologically informed model might be justified for univariate traits [5,7,9], there is a wealth of evidence showing that the evolution of complex multivariate phenotypes, such as the mammalian skull, follow rules of growth and inheritance that can be modelled using quantitative genetics theory [8,10]. Complex morphological traits are composed of subunits that are interconnected to each other to varying degrees. These different degrees of interconnection, generated by the complex interaction of multiple ontogenetic pathways, lead to an unequal variance distribution among parts, resulting in constraints to adaptive evolution [1,3,11]. Ignoring the possible role of constraints on the evolution of morphology can have many potential drawbacks, including establishing unrealistic expectations for drift in certain directions of the morphospace [3] and possibly obscuring the signal of directional selection. To investigate the effect of directional selection on macroevolutionary scales while avoiding potential pitfalls inherent to the analysis of multivariate traits, one should aim to study a complex trait with a well-known trait covariance structure and that probably experienced high rates of evolutionary change. One such example is the case of the evolution of the glyptodont skull.

Glyptodonts originated in South America and are members of the order Cingulata (Xenarthra, Mammalia), which includes the extant armadillos. An emblematic characteristic of glyptodonts that is shared with all members of this order is the presence of an osteoderm-based exoskeleton. However, glyptodonts can present a set of unique traits that makes them stand out from all other mammals, including defensive tail weaponry, large size, and, specifically, a highly modified skull. The glyptodont skull has undergone a particular process of telescoping in which the rostrum is ventrally expanded, and the tooth row is posteriorly extended, resulting in a structure with unprecedented biomechanical proprieties among mammals [12,13]. Because of this unique morphology, glyptodonts' phylogenetic position has been historically uncertain. While classically they have been regarded as a sister group to extant armadillos, recent ancient DNA analysis support that glyptodonts are nested within the extant armadillo clade, having originated during the late Miocene [14,15] (figure 2). As such, glyptodonts evolved during the same period it took for different extant armadillo lineages to diversify, making this a perfect model to study morphological evolution in a restricted taxonomic scope. Furthermore, the covariance structure of cranial traits has been extensively investigated in mammals in general and in Xenarthra specifically [16], allowing one to examine the evolution of cranial morphology in glyptodonts while considering the potential constraining effects of among-traits integration.

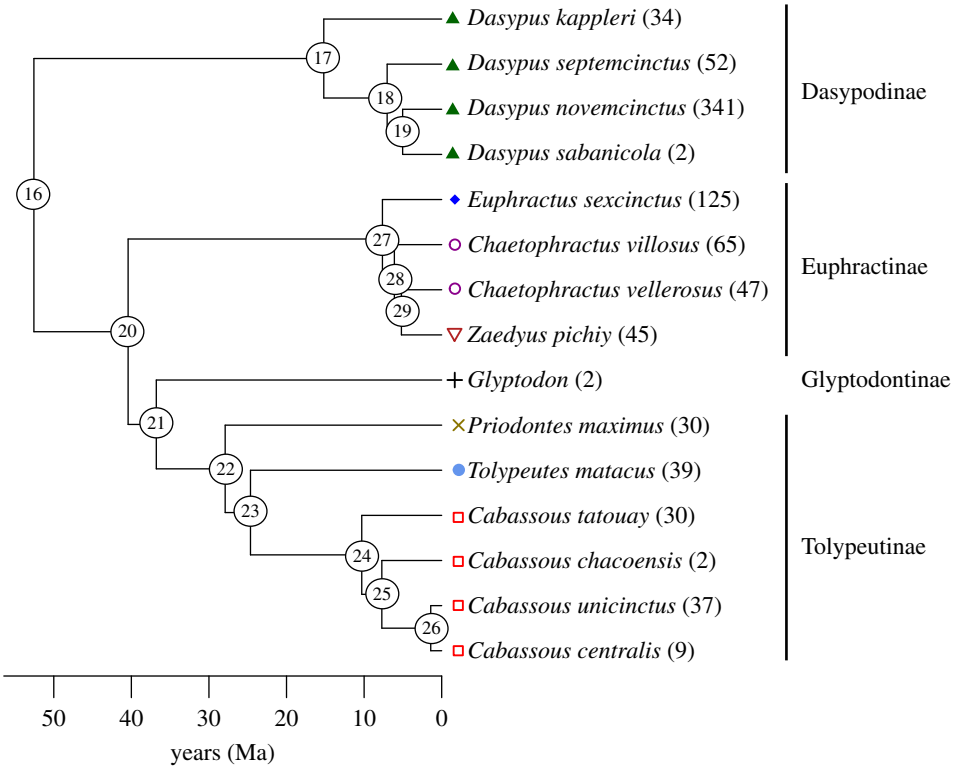

Figure 2. Cingulata phylogeny used in the present study based on [14]. Numbers within circles represent the node names referred throughout our manuscript. Colours and symbols are used in plot results. Numbers between parenthesis are each species sample sizes. (Online version in colour.)

The present contribution aims to use the unique glyptodont case to evaluate if we can identify the signal of directional selection on multivariate macroevolutionary data using biologically informed models of morphological evolution. Specifically, we calculate the empirical rates of evolution among Cingulata taxa and compare that to the expected rates of change under genetic drift to identify cases of morphological evolution that can be confidently associated with directional selection. Additionally, we retrospectively estimate the selective forces necessary to generate all morphological diversification within Cingulata to understand better if evolutionary processes responsible for the evolution of glyptodonts are qualitatively different (i.e., selection guided glyptodonts in different directions) from those associated with other Cingulata taxa.

2. Material and methods

(a) Morphometrics and trait covariance

Morphometric analysis was based on 33 linear distances obtained from three-dimensional cranial landmarks (electronic supplementary material, figure S1) digitized from 860 museum collection specimens (electronic supplementary material, table S1). These measurements are designed to capture general dimensions of bones and structures of the mammalian skull. Furthermore, the similarity between phenotypic and genotypic patterns of variation for these measurements has been well established for multiple taxa, including Cingulata [16]. Landmarks and distances are based on [16]. Traits were log-transformed to normalize differences in variance due to scale differences. Sample sizes ranged from 2 to 341 per species (figure 2), but sample size heterogeneity did not affect our covariance estimations (see electronic supplementary material). We adopted the phenotypic covariance matrix (or $\boldsymbol{P}$) as a surrogate of the additive genetic covariance matrix $\boldsymbol{G}$ (see [16] for details).

Here, we calculated $\boldsymbol{P}$ as the pooled within-group covariance matrix for all species. This assumes that the $\boldsymbol{P}$ is stable throughout the group's evolution [16]. Expressly, we assume that the $\boldsymbol{P}$ for glyptodonts is the same as for the rest of Cingulata. While this might be contentious due to the extreme morphological modification in the group, $\boldsymbol{P}$s were shown to be similar among extant and fossil Xenarthra, including giant ground sloths [16].

Form (shape + size) was quantified as the full morphospace of log-transformed variables, and size was measured as the geometric mean of all traits for each individual. Shape was quantified by removing the variation in form explained by size variation at the intraspecific level. This was done using a multivariate linear model using species and size as factors. Residuals from this model are shape variables free from the effect of size and allometry. Different shape quantifications did not change our interpretations (see electronic supplementary material), so we focus on the one described above for brevity. Morphological variation for form (the full morphospace) was represented with a principal component analysis (PCA).

(b) Reconstruction of past selection

To inspect if the selective pressures necessary to generate a glyptodont morphology differ from the remaining Cingulata in scale and direction (i.e., which combination of traits are favoured by natural selection), we calculated the selection gradients (βs) necessary to generate all divergence observed in our sample [9,11] using a version of the multivariate Breeder's equation

$$\beta = \boldsymbol{G}^{-1}\Delta z \tag{2.1}$$

with Δz being the phenotypic evolution that happened during a period of time. Here, we estimated Δz as the time-standardized phylogenetic-independent contrasts (PIC) obtained at each node [17,18], ensuring that β obtained like this are also phylogenetically independent from each other [19].

We applied an extension on eigenvalues after the 21st to minimize the effect of noise in the calculation of β [20] (see electronic

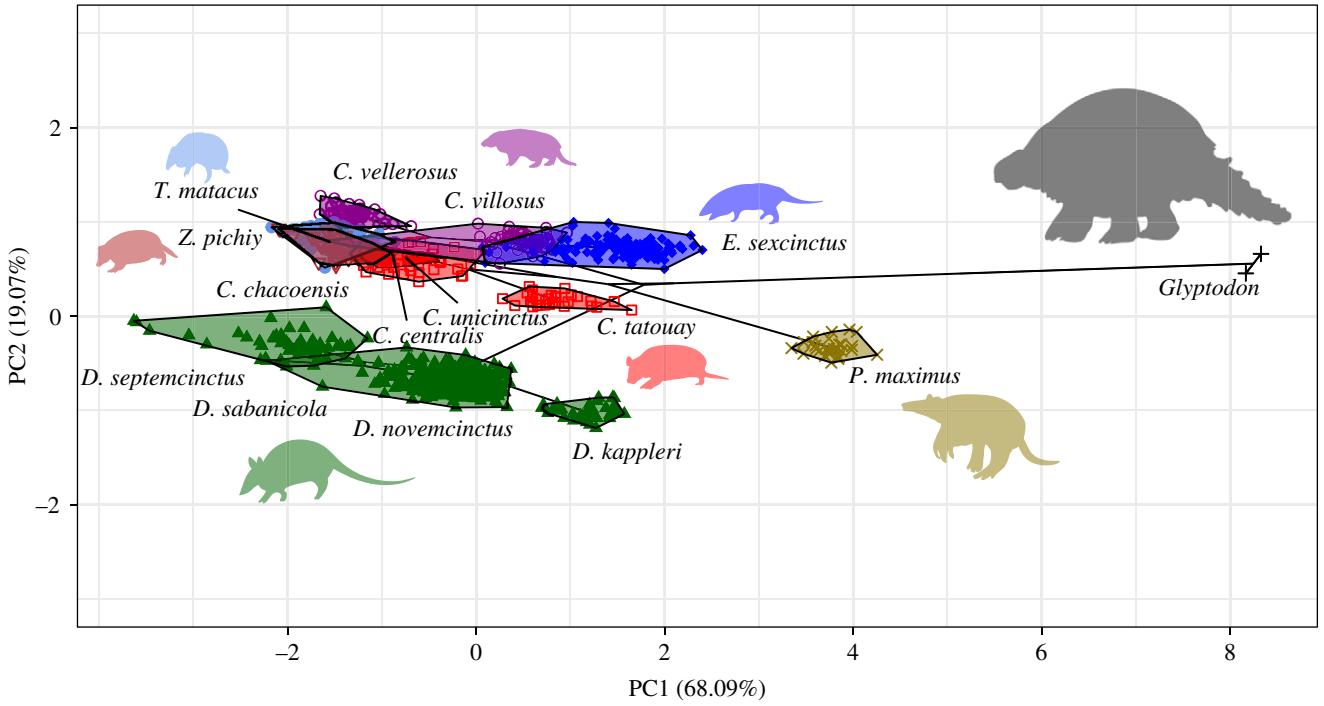

Figure 3. PCA of the 33 morphometric measurements of the skull of Cingulata species. Convex polygons encapsulate each species. Symbols and colours identify genus as shown in figure 2. (Online version in colour.)

supplementary material, figure S5). To summarize multiple βs, we performed an analysis similar to PCA, in which node-wise βs are projected on the leading lines of most selection. This was done by calculating the matrix of average cross-product of βs (the matrix of covariance of realized adaptive peaks), extracting the leading eigenvectors from that matrix, and projecting individual βs on the subspace defined by these axes [19]. The number of leading vectors was evaluated employing a simulation approach [19] (see electronic supplementary material).

(c) Mode of evolution

To evaluate the evolutionary processes involved in generating these morphological patterns, we employed Lande's generalized genetic distance (LGGD), which allows confronting observed rates of evolution to the expected rate under genetic drift while taking into account the genetic association (covariances) among traits [1]. The LGGD is calculated as

$$\mathrm{LGGD} = \frac{N_e}{t}\,\Delta z\, \boldsymbol{G}^{-1}\Delta z, \tag{2.2}$$

where t is the time in generations and N_e is the effective population size. LGGDs were obtained for form, allometry-free shape features and size.

For this analysis, the phylogeny was scaled, so the divergence time is given in generations instead of Myr. Generation times were set to be equal to the timing of sexual maturity of females plus the incubation period without assuming any reproductive seasonality. This is considered a conservative estimate, as these generation times are likely underestimated, leading to lower rates of evolution. Nevertheless, relaxing some of these assumptions (e.g., assuming seasonality or higher generation times) did not change our results (not shown). To obtain generation times for species without data on life-history traits (fossil species included), we estimated the linear relationship (in log scale) between body mass and generation time for 805 mammal species [21] and used the results to estimate the missing data. Because Cingulata shows a proportionally shorter generation time than the linear trend for all mammals, we subtracted a constant to correct for that difference (electronic supplementary material, figure S2). Given that *Glyptodon* body mass estimates can vary, ranging from 819 kg to 2000 kg [13,22], we calculated generation times for these extreme values. This resulted in generation times estimates ranging from 3.8 to 4.6 years, consistent with generation times for large ungulates [21,23]. Finally, to scale the phylogeny, we reconstructed ancestral values for generation time using maximum likelihood [24]. Each branch length was then divided by the average between the ancestral and descendent generation times. PIC values obtained in the scaled phylogeny are given in units $\Delta z/t$.

Since there is little available information for the N_e of Cingulata, we sampled N_e values from a uniform distribution ranging from 10 000 to 300 000. Estimates of effective population sizes for other Late Quaternary large herbivores range from 15 000–790 000 [23], so the values chosen here can be seen as conservative estimates in the case of glyptodonts. To approximate $\boldsymbol{G}$, we employed the Cheverud Conjecture [25], which states that the pattern of phenotypic covariances $\boldsymbol{P}$ can be used as a proxy for $\boldsymbol{G}$ when certain conditions are met [16]. Because $\boldsymbol{P}$s contain more variance than $\boldsymbol{G}$s, we scaled the latter according to a constant which, in the case of perfect proportionality between matrices, is equal to the average heritability ($\overline{h^2}$) of all traits [8]. Values for $\overline{h^2}$ were drawn from a uniform distribution ranging from 0.3 and 0.6, which are compatible with heritability estimates for the same cranial traits in other mammalian species [26,27]. Thus, we produced a range of LGGD values for each node to account for uncertainty on both N_e and $\overline{h^2}$.

Because parametric methods had an inadequate type I error rate (see electronic supplementary material, figure S3), a null distribution of LGGD was constructed by simulating multivariate evolution under genetic drift as follows

$$\boldsymbol{B} = \frac{t}{N_e}\boldsymbol{G}, \tag{2.3}$$

where $\boldsymbol{B}$ is the covariance matrix between evolutionary changes [1]. For each simulation, the randomly generated value of N_e was used to construct a $\boldsymbol{B}$ from which one observation would be drawn for one generation ($t = 1$). This procedure was repeated 10 000 times to generate a null distribution under drift. Values below 2.5% of the simulated values are considered to be dominated by stabilizing

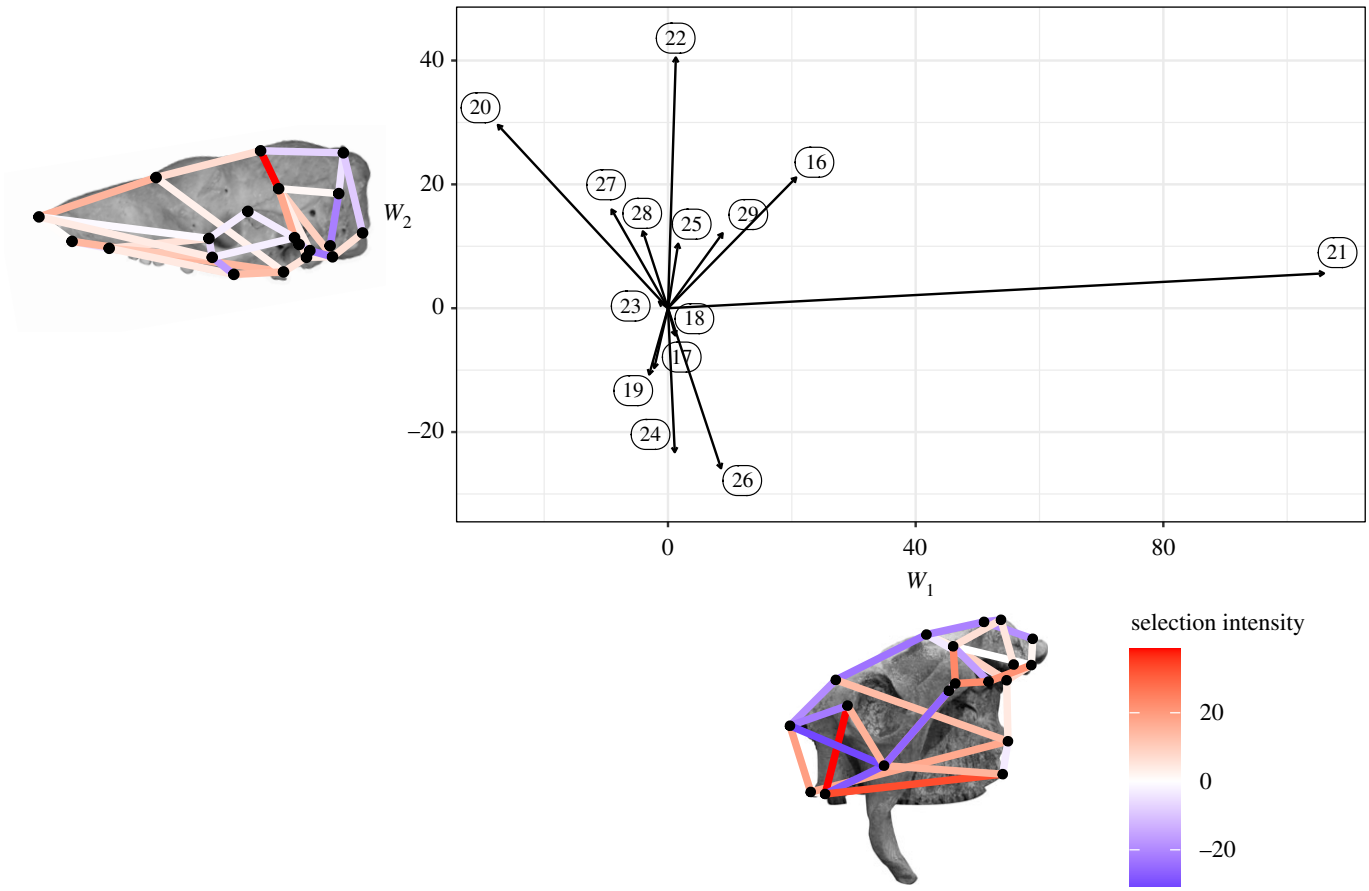

Figure 4. Projection of node-wise selection gradients on the two main predominant directions of directional selection (W_1 and W_2). Numbers represent the nodes on the phylogeny (figure 3*a*). Skulls depict a graphical representation of the two main directions W_1 (*Glyptodon* skull) and W_2 (*Cabassous* skull). Colours represent the intensity and direction (blue-negative and red-positive) of selection. (Online version in colour.)

selection, and values above 97.5% of the simulated values are considered to be dominated by directional selection (figure 1). Note that estimated rates in a macroevolutionary context are better seen as the net effect of the sum of all evolutionary processes that acted during the history of a lineage. Thus, instead of classifying lineages under either directional or stabilizing selection (or drift), our results should be seen as an investigation of the relative importance of these multiple processes.

3. Results

(a) Morphometrics and past selection

The PCA of our full multivariate dataset of skull measurements illustrates the uniqueness of Glyptodontinae morphology (figure 3). Glyptodontinae shows an extreme score on PC1 compared to the extant armadillos, which is considered a size and allometric direction (electronic supplementary material, table S2) and explains 68.09% of the total variation. The giant armadillo *Priodontes maximus* also presents a high score on PC1, but with values still closer to the remaining Cingulata than to *Glyptodon*. Dasypodidae species tend to occupy a different position of the morphospace than Euphractinae and Tolypeutinae, with similar PC1 values but smaller PC2 scores. The PC2 explains 19.07% of the variation and is associated with an increase in the size of facial traits (electronic supplementary material, table S2). The remaining PCs explained less than 5% of the total variation.

The simulation approach was designed to identify how many directions of preferential selection are necessary to produce the morphological diversity in Cingulata recovered the first three leading eigenvectors of the covariance matrix of selection gradients (W_1, W_2 and W_3) as significant (electronic supplementary material, figure S6). The leading vector W_1 summarizes selection for reducing the skull's total length while also showing a dorsoventral expansion of the face region, along with an increase in the tooth-row size (figure 4). The only node that scores heavily on this axis is associated with the origin of glyptodonts (node 21), suggesting that this is a glyptodont-exclusive combination of selective pressures. The second axis W_2 summarizes a contrast between face and neurocranium. The nodes with the highest scores on this axis, 20 and 22, neighbour the node leading to glyptodonts, while the ones with the lowest scores, 24 and 26, are nodes internal to the *Cabassous* genus. The third axis W_3 shows strong selection of features associated with the skull height (electronic supplementary material, figure S7). An inspection of the scores along with W_3 reveals that this axis is mostly associated with the differentiation within Euphractinae (nodes 27—29).

(b) Mode of evolution

LGGD shows that stabilizing selection was the dominant force in the morphological evolution of Cingulata, a fact that is more evident for both form and shape (figure 5*a*,*b*). For size, most observed LGGD values fell within the expected under drift (figure 5*c*). While most nodes failed to exhibit values above the expected under drift, a noticeable exception was the one representing the divergence between

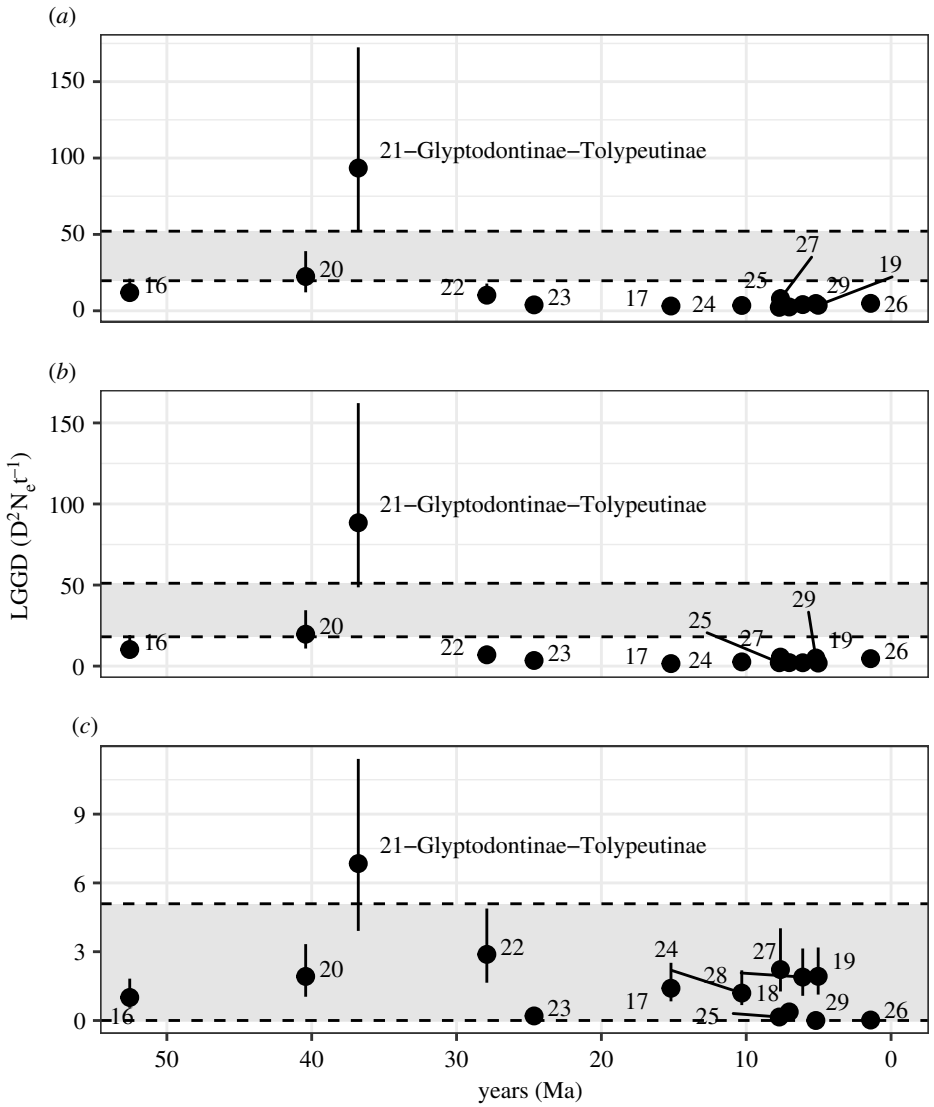

Figure 5. Values for LGGD for each node plotted against node age for form (*a*), shape (*b*) and size (*c*). Dots and solid lines represent the median and the ranges for the LGGD values for a given node. Nodes are numbered following figure 3*a*. The grey area represents the expectation under drift. Values above it are consistent with directional selection and below it with stabilizing selection. (Online version in colour.)

Glyptodontinae and Tolypeutinae (node 21). This node presented LGGD values for form, shape and size that fall above the expected under drift, suggesting that directional selection had a pre-eminent role during the divergence of this group. The multivariate PIC for this node and PC1 of the full dataset (figure 3) are highly aligned (vector correlation greater than or equal to 0.98), indicating that this direction is mostly associated with the divergence of glyptodonts from all remaining Cingulata. The increased evolutionary rate observed for this node does not seem to be an artefact introduced by the timing of the origin of glyptodonts, as older nodes associated with the divergence of subfamilies within Cingulata did not show elevated LGGD values (figure 5).

4. Discussion

Previous investigations on the macroevolutionary rates of morphological evolution in mammals have shown that morphological change is orders of magnitude slower than would be expected by drift [5]. Such macroevolutionary rates are usually measured as the ratio between total morphological differentiation and time [17]. As divergence times increase, even extreme changes can get diluted, implying that searching for signals of directional selection in macroevolutionary data might be futile (figure 1). In this sense, our analysis produces a more nuanced understanding of such a process.

Broadly speaking, our results agree with previous evidence that stabilizing selection is the dominant evolutionary process shaping mammalian morphological diversification [5,7,8]. Rates of morphological evolution calculated throughout the evolutionary history of Cingulata are consistent with stabilizing selection, a pattern that is more expressive for shape than for size [4]. This finding is in line with previous suggestions that shape features are more constrained than size, implying that the former is more affected by stabilizing selection than the latter [28]. One proposed explanation for this pattern refers to the macroevolutionary dynamic of adaptive zones [29]. Adaptive zones are regions of the phenotypic space defined by a specific ecomorphological association between phenotype, function and ecology. Within that region, evolution typically results in quantitative differences in ecology and morphology. The escape of such a region and the invasion of a new

adaptive zone is usually associated with more extreme changes in morphology and ecology, a feature observed in major evolutionary transitions and innovations [29]. If, as some have suggested, shape features are more strongly associated with functional demands (e.g., [30–34]), then qualitative changes in ecomorphological requirements, such as those derived from ecological shifts, would probably lead to shape evolution and possibly to the invasion of a new adaptive zone [19,32]. Size changes without accompanying shape changes, on the other hand, are less likely to impact form–function relationships, being associated with within-zones change [19,32]. In fact, most of the evolution of Cingulata seems to concentrate on a similar region of the morphospace (figure 3). If the morphospace occupation of the extant species is representative of the selective pressures determining morphological evolution for this group, then this pattern can be construed as evidence that their morphology is being maintained within a 'generalist-armadillo' adaptive zone [30]. Within that zone, shape and size would be under strong stabilizing selection, but size would be more prone to change. This interpretation is reinforced by the fact that there is no clear relationship between size and shape at the macroevolutionary scale for armadillos (electronic supplementary material, figure S8), suggesting that both features are relatively decoupled, with maybe the exception of Tolypeutinae.

The only exception to this rule, both in terms of morphospace occupation and rates of evolution, is the glyptodont lineage (figures 3 and 5). Glyptodonts seem to have reached a region unoccupied by other Cingulata (figure 3). The most straightforward explanation for this is that glyptodonts invaded a new adaptive zone fuelled by a drastic change in ecology. Glyptodonts are thought to be highly specialized herbivores, a diet with strong functional demands [13]. These demands were then responsible for imposing a strong directional selection, leading to radical morphological change and functional innovation seen in this group [12]. The investigation of hypothetical past selection further reinforces this interpretation. The description of W_1, which is a glyptodont-exclusive axis, matches the telescoping process that glyptodonts went through during their evolutionary history [12]. Furthermore, the required strength of selection for the divergence of glyptodonts is superior to those observed within the generalist-armadillo adaptive zone. Changes in the orientation and strength of selection have been associated with dietary shifts in other mammals [19,35], reinforcing this idea that the selective change observed in glyptodonts has an ecomorphological basis.

The fact that the signal of directional selection is detectable in a macroevolutionary scale is remarkable. To our knowledge, a comparable signal was only previously found at the divergence between lower and higher apes, at 20 Ma, and at the origin of humans, at 6 Ma [8]. This is somewhat expected, as primates are marked by a phylogenetic trend towards increased brain size, a pattern that is intensified on hominins [34,36]. It is possible that a trend of continuous differentiation also marked the evolution of Glyptodontinae. Early representatives of the group, such as *Propalaehoplophorus*, exhibit an intermediary version of the cranial telescoping characteristic of latter glyptodonts [12]. Given that the split between Glyptodontinae and Tolypeutinae happened 35 Ma ago [14,15] and *Propalaehoplophorus* is known from the fossil record from 22 to 15 Ma [37], then it is likely that the accumulation of morphological changes in this lineage was probably gradual. If that is the case, then glyptodonts can be the oldest and longest case of such a pattern of continuous change. Alternatively, if the group's evolution was punctuated by long periods of stasis, this could mean that directional selection events were even more intense than shown by the present analysis (figure 1). However, given the clear difference between primitive and derived forms within the group, the truth probably lies somewhere in between, with a gradual directional evolution punctuated by some periods of stasis but in proportions that differ from the remaining Cingulata and even other mammals.

The extent to which the evolution of the glyptodont morphology is associated with size is unclear. While the evolution of both a different morphology and large body size are probably causally related in glyptodonts, changes in the group do not seem to be a consequence of extrapolations of a Cingulata allometric pattern (electronic supplementary material, figure S8). Furthermore, because early glyptodonts were considerably smaller than the specimens investigated here [37], the evolution of the extreme adaptations seen in this group can be relatively decoupled from size, as reinforced by the lack of any strong signal of size selection in either glyptodonts and Cingulata as a whole (figure 4). However, size evolution could have triggered large-scale reformulations of morphology in response to new demands imposed by an increased size [19]. A more nuanced view of the role of size in the group's evolution would benefit from a thorough investigation of fossil representatives from Cingulata.

As mentioned above, the use of biologically informed models to investigate evolutionary rates at macroevolutionary scales is still rare and limited in scope. We suggest that some of this dismissal comes from the assumed inapplicability of these models at larger timescales due to the overwriting power of stabilizing selection. Here, we show that this assumption does not hold for glyptodonts, suggesting that directional selection is more pervasive than previously thought. The integration of more refined palaeontological, demographic and life-history data in the investigation of macroevolutionary questions can lead to a more nuanced view of the role of directional and stabilizing selection on the evolution of complex morphologies.

Data accessibility. All data and R scripts necessary to reproduce the present results are available in the electronic supplementary material [38].

Authors' contributions. F.A.M.: conceptualization, data curation, formal analysis, investigation, methodology, software, visualization, writing—original draft and writing—review and editing; A.H.: conceptualization, data curation, formal analysis, funding acquisition, investigation, methodology, project administration, validation, visualization, writing—original draft and writing—review and editing; G.M.: conceptualization, funding acquisition, investigation, methodology, project administration, resources, supervision, validation and writing—review and editing.

All authors gave final approval for publication and agreed to be held accountable for the work performed therein.

Competing interests. We declare we have no competing interests.

Funding. This work was partially supported by grants from NSF to F.A.M. (DEB 1350474 and DEB 1942717) and FAPESP to A.H. and G.M. (2012/24937-9; 2011/14295-7).

Acknowledgements. We thank the curators of the following institutions for providing access to specimens and support for data acquisition: American Museum of Natural History; California Academy of Science; Faculdad de Ciencias de la Universidad de la Republica; Field Museum of Natural History; Museu Paraense Emílio Goeldi; Idaho Museum of Natural History; Los Angeles County Museum; La Brea Tar Pits and Museum; Museo Argentino de Ciencias Naturales; Museu de Ciências Naturais da Pontifícia Universidade Católica de Minas Gerais; Museu de Ciências Naturais da Fundação

Zoobotânica do Rio Grande do Sul; Museo de La Plata; Museo Paleontológico de Colonia del Sacramento; Museu Nacional de Historia Natural de Montevideo; Museu Nacional (Rio de Janeiro); University of California Museum of Vertebrate Zoology; Natural History Museum (London); University of California Museum of Paleontology; Florida Museum of Natural History; Smithsonian National Museum of Natural History; Museu de Zoologia da Universidade de São Paulo; Universidade Federal do Piauí. We also thank EvoClub_BR discussion group and the members of Uyeda's Lab (Virginia Tech) for thoughtful comments and suggestions to the text. We thank two anonymous reviewers for their comments and suggestions and M. C. Luna for kindly producing the silhouettes used here.

References

1. Lande R. 1979 Quantitative genetic analysis of multivariate evolution, applied to brain: body size allometry. *Evolution* **33**, 402–416. (doi:10.1111/j.1558-5646.1979.tb04678.x)
2. Turelli M, Gillespie JH, Lande R. 1988 Rate tests for selection on quantitative characters during macroevolution and microevolution. *Evolution* **42**, 1085–1089. (doi:10.1111/j.1558-5646.1988.tb02526.x)
3. Hansen T, Houle D. 2008 Measuring and comparing evolvability and constraint in multivariate characters. *J. Evol. Biol.* **21**, 1201–1219. (doi:10.1111/j.1420-9101.2008.01573.x)
4. Leinonen T, McCairns RS, O'hara RB, Merilä J. 2013 Q_{ST} -f_{ST} comparisons: evolutionary and ecological insights from genomic heterogeneity. *Nat. Rev. Genet.* **14**, 179–190. (doi:10.1038/nrg3395)
5. Lynch M. 1990 The rate of morphological evolution in mammals from the standpoint of the neutral expectation. *Am. Nat.* **136**, 727–741. (doi:10.1086/285128)
6. Lande R. 1986 The dynamics of peak shifts and the pattern of morphological evolution. *Paleobiology* **12**, 343–354. (doi:10.1017/S0094837300003092)
7. Lemos B, Marroig G, Cerqueira R. 2001 Evolutionary rates and stabilizing selection in large-bodied opossum skulls (Didelphimorphia: Didelphidae). *J. Zool.* **255**, 181–189. (doi:10.1017/S095283690100125X)
8. Schroeder L, von Cramon-Taubadel N. 2017 The evolution of hominoid cranial diversity: a quantitative genetic approach. *Evolution* **71**, 2634–2649. (doi:10.1111/evo.13361)
9. Grabowski M, Roseman CC. 2015 Complex and changing patterns of natural selection explain the evolution of the human hip. *J. Hum. Evol.* **85**, 94–110. (doi:10.1016/j.jhevol.2015.05.008)
10. Marroig G, Cheverud JM. 2004 Did natural selection or genetic drift produce the cranial diversification of neotropical monkeys? *Am. Nat.* **163**, 417–428. (doi:10.1086/381693)
11. Marroig G, Cheverud JM. 2010 Size as a line of least resistance II: direct selection on size or correlated response due to constraints? *Evolution* **64**, 1470–1488.
12. Fariña RA, Vizcaíno S. 2001 Carved teeth and strange jaws: how glyptodonts masticated. *Acta Palaeontol. Polonica* **46**, 219–234.
13. Vizcaíno SF, Cassini GH, Fernicola JC, Bargo MS. 2011 Evaluating habitats and feeding habits through ecomorphological features in glyptodonts (Mammalia, Xenarthra). *Ameghiniana* **48**, 305–319. (doi:10.5710/AMGH.v48i3(364))
14. Delsuc F *et al.* 2016 The phylogenetic affinities of the extinct glyptodonts. *Curr. Biol.* **26**, R155–R156. (doi:10.1016/j.cub.2016.01.039)
15. Mitchell KJ, Scanferla A, Soibelzon E, Bonini R, Ochoa J, Cooper A. 2016 Ancient DNA from the extinct South American giant glyptodont *Doedicurus* sp. (Xenarthra: Glyptodontidae) reveals that glyptodonts evolved from Eocene armadillos. *Mol. Ecol.* **25**, 3499–3508. (doi:10.1111/mec.13695)
16. Hubbe A, Melo D, Marroig G. 2016 A case study of extant and extinct Xenarthra cranium covariance structure: implications and applications to paleontology. *Paleobiology* **42**, 465–488. (doi:10.1017/pab.2015.49)
17. Felsenstein J. 1985 Phylogenies and the comparative method. *Am. Nat.* **125**, 1–15. (doi:10.1086/284325)
18. Felsenstein J. 1988 Phylogenies and quantitative characters. *Annu. Rev. Ecol. Syst.* **19**, 445–471. (doi:10.1146/annurev.es.19.110188.002305)
19. Machado FA. 2020 Selection and constraints in the ecomorphological adaptive evolution of the skull of living Canidae (Carnivora, Mammalia). *Am. Nat.* **196**, 197–215. (doi:10.1086/709610)
20. Marroig G, Melo DAR, Garcia GRG. 2012 Modularity, noise, and natural selection. *Evolution* **66**, 1506–1524. (doi:10.1111/j.1558-5646.2011.01555.x)
21. De Magalhaes J, Costa J. 2009 A database of vertebrate longevity records and their relation to other life-history traits. *J. Evol. Biol.* **22**, 1770–1774. (doi:10.1111/j.1420-9101.2009.01783.x)
22. Vizcaíno SF, Blanco RE, Bender JB, Milne N. 2010 Proportions and function of the limbs of glyptodonts. *Lethaia* **44**, 93–101. (doi:10.1111/j.1502-3931.2010.00228.x)
23. Lorenzen ED *et al.* 2011 Species-specific responses of Late Quaternary megafauna to climate and humans. *Nature* **479**, 359–364. (doi:10.1038/nature10574)
24. Schluter D, Price T, Mooers AØ, Ludwig D. 1997 Likelihood of ancestor states in adaptive radiation. *Evolution* **51**, 1699–1711. (doi:10.1111/j.1558-5646.1997.tb05095.x)
25. Cheverud JM. 1988 A comparison of genetic and phenotypic correlations. *Evolution* **42**, 958–968. (doi:10.1111/j.1558-5646.1988.tb02514.x)
26. Garcia GRG, Hingst-Zaher E, Cerqueira R, Marroig G. 2014 Quantitative genetics and modularity in cranial and mandibular morphology of *Calomys expulsus*. *Evol. Biol.* **41**, 619–636. (doi:10.1007/s11692-014-9293-4)
27. Porto A, Sebastião H, Pavan SE, VandeBerg JL, Marroig G, Cheverud JM. 2015 Rate of evolutionary change in cranial morphology of the marsupial genus *Monodelphis* constrained by the availability of additive genetic variation. *J. Evol. Biol.* **28**, 973–985. (doi:10.1111/jeb.12628)
28. Clyde WC, Gingerich PD. 1994 Rates of evolution in the dentition of early Eocene *Cantius*: comparison of size and shape. *Paleobiology* **20**, 506–522. (doi:10.1017/S0094837300012963)
29. Simpson GG. 1944 *Tempo and mode in evolution*. New York: NY: Columbia University Press.
30. Polly PD. 2008 Adaptive zones and the pinniped ankle: a three-dimensional quantitative analysis of carnivoran tarsal evolution. In *Mammalian evolutionary morphology*, pp. 167–196. Berlin, Germany: Springer.
31. Machado FA, Hubbe A, Melo D, Porto A, Marroig G. 2019 Measuring the magnitude of morphological integration: the effect of differences in morphometric representations and the inclusion of size. *Evolution* **33**, 402–411.
32. Slater GJ, Friscia AR. 2019 Hierarchy in adaptive radiation: a case study using the Carnivora (Mammalia). *Evolution* **73**, 524–539. (doi:10.1111/evo.13689)
33. Mitchell DR, Sherratt E, Ledogar JA, Wroe S. 2018 The biomechanics of foraging determines face length among kangaroos and their relatives. *Proc. R. Soc. B* **285**, 20180845. (doi:10.1098/rspb.2018.0845)
34. Sansalone G *et al.* 2020 Variation in the strength of allometry drives rates of evolution in primate brain shape. *Proc. R. Soc. B* **287**, 20200807. (doi:10.1098/rspb.2020.0807)
35. Rossoni DM, Assis APA, Giannini NP, Marroig G. 2017 Intense natural selection preceded the invasion of new adaptive zones during the radiation of new world leaf-nosed bats. *Sci. Rep.* **7**, 11076. (doi:10.1038/s41598-017-08989-6)
36. Melchionna M *et al.* 2020 Macroevolutionary trends of brain mass in primates. *Biol. J. Linn. Soc.* **129**, 14–25.
37. Fernicola JC. 2008 Nuevos aportes para la sistemática de los Glyptodontia Ameghino 1889 (Mammalia, Xenarthra, Cingulata). *Ameghiniana* **45**, 553–574.
38. Machado FA, Marroig G, Hubbe A. 2022 The pre-eminent role of directional selection in generating extreme morphological change in glyptodonts (Cingulata; Xenarthra). Figshare.